https://doi.org/10.48047/AFJBS.6.2.2024.2612-2627

African Journal of Biological Sciences

Journal homepage: http://www.afjbs.com

Research Paper Open Access

Right Ventricular function assessment and Pulmonary Hypertension in Children with Pneumonia

Eman Abdel Raheem Yusef, Tarek Mohamed Atteia, Nehad Ahmed Karam, Al Shaymaa Ahmed Ali

Pediatrics Department, Faculty of Medicine, Zagazig University

Corresponding author: Eman Abdel Raheem Yusef

Email: emy.abdelreheem@gmail.com

Article History

Volume 6, Issue 2, Apr-Aug 2024

Received: 10 August 2024

Accepted: 30 August 2024

Published: 30 August 2024

doi: 10.48047/AFJBS.6.2.2024.2612-2627

Abstract: RV enlargement may be caused by states of acute or chronic pressure overload, chronic volume overload, or intrinsic myocardial pathology, often indicating severe and/or advanced disease with a relatively poor prognosis. The infant RV has limited capability to adapt to different loading conditions associated with pneumonia and acute respiratory failure as compared to adults. The accurate assessment of RV size and functions is important in the management, and prognostication of these conditions. A reliable echocardiographic evaluation of the RV systolic and diastolic dysfunction is challenging owing to its complex morphology, and different physiology compared to the left ventricle. This review provides an approach to assessing a combination of different parameters of RV function and pulmonary hypertension in children with pneumonia and respiratory failure. The area of the body and apex of the RV is measured by planimetry of the RV cavity in the apical four-chamber view at end-diastole (when the RV cavity is at its largest). When tracing the endocardial contour, care must be taken to trace along the true border of the RV wall not the prominent trabeculations. RV linear, basal and mid-cavity dimensions also are measured in the apical four-chamber view using the RV-focused view. RV volume 2D estimates of RV volume are not recommended due to their inherent geometric assumptions and lack of full representation of the different RV regions (often resulting in substantial underestimation of true RV volume). However, 3D measures of RV volume have largely overcome these limitations and can be obtained using 3D surface modeling platforms that can calculate global and regional RV volumes. For children and infants, the definition of PH is the same as in adults: mean pulmonary artery pressure (PAP) >20 mmHg at sea level. Virtually all types of Pulmonary Hypertension can be observed in pediatric patients. The most common types of persistent/progressive PH in children are PH associated with congenital heart disease, PH due to lung disease, and idiopathic/heritable PH. PH is well described in children with collagen vascular disease, liver disease, and acute thromboembolism, but these diseases are rare causes of PH in children. Estimation of pulmonary artery pressure (PAP) is an important component of the echocardiographic study; in this review we highlight the different ways to assess pulmonary hypertension.

Keywords: *Right Ventricular function, Pulmonary Hypertension, Children*

Introduction

Childhood pneumonia is an important cause of morbidity in resource-rich countries, and mortality in resource-limited countries. Pneumonia represents any inflammatory condition involving the lungs, which include the visceral pleura, connective tissue, airways, alveoli, and vascular structures. Pneumonia is defined as a condition typically associated with fever, respiratory symptoms, and evidence of parenchymal involvement, either by physical examination or the presence of infiltrates on chest radiography [1].

Despite the RV dysfunction and pulmonary hypertension being a described phenomenon in the scope of adult literature, evidenced by multiple reviews on this topic in recent years [2], there is a scarcity in literature addressing the topic of RV and pulmonary hypertension in pneumonia or acute respiratory failure in children. The purpose of this narrative review is to raise a greater awareness of the presence of this under-recognized and often-neglected right heart to the pediatric critical care physicians and researchers and improve our understanding of mechanisms driving this disease and the different methods to assess this disease especially by echocardiography. That can substantially improve outcomes in these children.

In the setting of acute lung injury, either due to the original disease or in the ventilated babies with the recommended guidelines in pediatrics acknowledging the importance of lung-protective strategies, the resulting hypoxemia, hypercapnia, and acidemia, along with disturbance of lung architecture from partial atelectasis or alveolar overdistention, elevates pulmonary vascular resistance (PVR) and RV afterload that appears to be potentially hazardous for children with limited capacity to handle acute changes in RV end-diastolic pressure (RVEDP) or volume (RVEDV) [3].

Respiratory Failure:

Respiratory failure is a condition in which the respiratory system fails in oxygenation or carbon dioxide elimination or both. There are 2 types of impaired gas exchange: (1) Hypoxemic respiratory failure, which is a result of lung failure, and (2) Hypercapnic respiratory failure, which is a result of respiratory pump failure [1]. In hypoxemic respiratory failure, alveolar ventilation-pulmonary perfusion (V/Q) mismatch results in the decrease of PaO2 to below 60 mm Hg with normal or low PaCO2. In hypercapnic respiratory failure, V/Q mismatch results in the increase of PaCO2 to above 50 mm Hg. Either hypoxemic or hypercapnic respiratory failure can be acute or chronic [2].

Laboratory and radiographic studies are helpful in the assessment of respiratory failure and the monitoring of the response to therapeutic management. Laboratory studies, such as an arterial blood gas, end-tidal carbon dioxide, oxygen saturation, a complete blood cell count with differential, and renal and liver functions, should be performed. The arterial blood gas accurately measures the extent of the gas exchange abnormality and confirms the type and chronicity of respiratory failure [2].

In chronic carbon dioxide retention, carbon dioxide is increased, pH is normal, and serum bicarbonate concentration and base excess are increased. The arterial blood gas of the patient with an opiate overdose differs based on the severity of the overdose. In mild to moderate opiate overdose, respiratory acidosis is observed with a pH below 7.35, PaCO2 greater than 50 mm Hg, and a low or normal serum bicarbonate concentration. In severe opiate overdose, a mixed respiratory and metabolic acidosis is observed. End-tidal carbon dioxide is measured from expired air from the nose by a capnometer and is a common and reliable tool used in the emergency department and critical care setting [3].

The complete blood cell count helps to assess such causes as infection, anemia, or polycythemia. In addition, respiratory, blood, urine, and pleural cultures and polymerase chain reaction can be performed when indicated to identify the specific bacterial cause. Renal and liver function tests provide clues to the cause of or identify complications associated with respiratory failure. Electrolyte abnormalities, such as hypernatremia or hyponatremia, cause seizures, and hyperkalemia causes cardiac arrhythmia [3].

Chest radiography should be performed in patients who present with respiratory failure to help identify or confirm the cause of the respiratory failure. If a cardiac cause of acute respiratory failure is suspected,

electrocardiography and echocardiography should be performed. Pulmonary function testing includes a group of tests, such as spirometry, lung volumes, diffusion capacity, and maximal respiratory pressures, among others. Pulmonary function testing evaluates the functional status of the respiratory system by measuring the volume and flow of air movement, gas exchange, and strength of the respiratory muscles. Biopsies and bronchoalveolar lavage for microbiologic, cytologic, and histologic testing can be obtained with bronchoscopy. Bronchoscopy and pulmonary function testing are not performed when the patient is critically ill [4].

Right Ventricular Function

Anatomy and Mechanics of Right Ventricle (RV):

The anatomy and physiology of the RV are both unique and complex and quite different from LV. In contrast to the ellipsoidal shape of the LV, the RV appears triangular and crescent-shaped. Anatomically, RV can be described regarding three components [4]: (1) The inlet, consists of the tricuspid valve, chordal tendineae, and papillary muscles; (2) The trabeculated apical myocardium; and (3) The infundibulum, or conus, which corresponds to the outlet region [5].

Regarding the myofiber architecture of the heart, the ventricular myocardium is constituted by a continuous band of muscle that extends from the pulmonary artery root to the aortic root, forming a helical structure with two spirals and delimiting the two ventricular cavities. This myocardial band would be composed of the "basal loop" and the "apical loop." The basal loop is predominantly horizontal and comprises the right and left segments; the apical loop is predominantly vertical and consists of a descending segment and an ascending segment [6, 7].

Under normal afterload, RV contraction begins at the sinus (inlet chamber) and progresses toward the conus or infundibulum (outlet chamber), indicating a pattern of contraction from apex to base [8].

The RV contracts by three mechanisms:

- Inward movement of the free wall secondary to the contraction of the right segment of the basal loop (transverse orientation), which produces a bellows effect,
- Contraction of the ascending segment of the apical loop (oblique orientation), which shortens the long axis, drawing the tricuspid annulus toward the apex; and
- Traction on the free wall at the points of attachment secondary to LV contraction [8].

The shortening of the RV is mainly longitudinal compared to radial. The low impedance and the high capacitance of the normal pulmonary circulation are reflected in the triangular shape of the RV pressure-volume loop, without distinct periods of isovolumic contraction and relaxation. RV ejection begins early during the increase of intraventricular pressure and continues during its fall. This prolonged low-pressure ejection implies that RV emptying is very sensitive to changes in afterload and that RV keeps on ejecting (late phase of ejection) while the LV is in diastole (isovolumic relaxation and rapid filling phases or pre suction and suction phases, resp.). It corresponds to the contraction of the ascending segment of the apical loop without opposition of the descending segment that is relaxed (named by Torrent-Guasp "late isovolumetric contraction") [8].

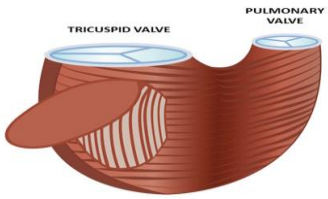

Figure (1): Schematic representation of the right ventricular myofiber orientation. On the epicardial surface, circumferentially oriented myofibers are present; these myofibers encompass the subpulmonary infundibulum

and advance more or less parallel with the atrioventricular groove. At the apex, this layer spirals into the deep layer of the RV. This subendocardial fiber orientation is rather longitudinal (as shown inside the cavity). [9]

Right Ventricular Mechanics:

Infant heart has lower contractile reserve compared to older children or adults: In the young infant heart cardiomyocyte and at the cell level, myocardial fibers have less number of organized myofibrils with higher connective tissue-to-contractile protein ratios. This myofibril anatomy decreases the ability of the cardiomyocyte to both contract and to relax, resulting in minimal systolic and diastolic reserve in children. Furthermore, the transverse tubules and sarcoplasmic reticula inside cardiomyocytes are also immature, restricting the calcium-dependent inotropic action of the infant's myocardium and making the myocardium dependant upon extracellular calcium for sarcomeric contraction. Moreover, the infant heart has higher parasympathetic innervation with lower β-adrenergic receptor expression [10].

RV has limited contractile reserve compared LV: These factors together limit RV contractile capacity and metabolic reserve at baseline in both neonates and younger children.

While LV has three layers of myocardial fiber with complex alignment allowing torsional constriction of the LV cavity, in contrast the density and anatomic arrangement of RV fibers is made of only superficial transversely aligned and deep layers of longitudinally aligned muscle fibers. The superficial myofibers blends into the superficial myocardial layer of the ventricular septum and LV [11]. RV myocardial fibers carries a significantly lower number of mitochondria [12].

In older children and adults, the RV has a better capability to withstand sudden high demands (increases in preload and afterload) by elevations in heart rate, contractility, and stretch to accommodate the increased RV end diastolic volume (RVEDV). In young infants, the resting heart rate is already high, thus, causing a narrow "therapeutic window" for compensatory elevation of heart rates and subsequently cardiac output, as significant tachycardia limits ventricular filling. Additionally, the PVR in some infants may remain elevated for the first several months of life, increasing basal afterload on the RV. In children with elevated PVR from birth as seen in bronchopulmonary dysplasia or congenital heart diseases with pulmonary over-circulation, the poorly compliant RV adapts to the high levels of wall stress by compensatory hypertrophy, furtherly limiting RV diastolic function [13].

Owing to the limited RV myocardium contractile reserve, acute increases in RVEDV are initially tolerated by mild dilation of RV wall. But greater stress by increasing afterload and/or preload result in marked dilatation and systolic function becomes embarrassed lowering stroke volume (extreme of the Frank–Starling relationship).

Ventricular interdependence: The acute RV dilation will encroach on the LV cavity through ventricular interdependence. In combination with diminished pulmonary venous return due to limited RV output and reduced pulmonary blood flow, LV compression can result in an embarrassment to systemic cardiac output—a process termed acute cor pulmonale. The combination of increased RV wall stress and decreased systemic cardiac output can result in coronary ischemia that further reduces RV systolic function that can culminate in cardiac arrest [14].

Right Ventricular Size:

RV enlargement may be caused by states of acute or chronic pressure overload, chronic volume overload, or intrinsic myocardial pathology, often indicating severe and/or advanced disease with a relatively poor prognosis [7].

For patients with repaired tetralogy of Fallot and residual-free pulmonary regurgitation, RV size is vigilantly monitored to determine the timing of pulmonary valve replacement. Although typically measured by cardiovascular magnetic resonance (CMR) to achieve high accuracy, reports suggest that 3D echocardiography provides similar measurements of RV volumes [10].

Right Ventricular Area:

The area of the body and apex of the RV is measured by planimetry of the RV cavity in the apical four-chamber view at end-diastole (when the RV cavity is at its largest). When tracing the endocardial contour, care must be taken to trace along the true border of the RV wall rather than the prominent trabeculations or moderator band [10].

Two common sources of error, resulting in underestimation of RV area, are:

- RV linear dimensions, RV linear dimensions are measured in the apical four-chamber view, ideally using the RV-focused view, at end-diastole. RV basal dimension, RV mid-cavity dimension (midway between the apex and tricuspid annular plane) [9].
- RVOT dimension The proximal RV outflow tract (RVOT) dimension is measured from the RVOT anteriorly to the aortic root posteriorly; it can be measured in the parasternal long-axis or parasternal short-axis view, The distal RVOT diameter, commonly used in the calculation of RV stroke volume, is measured just proximal to the insertion of the pulmonary valve leaflets in the parasternal short-axis [11].

Right Ventricular Volume

Two-dimensional estimates of RV volume are not recommended due to their inherent geometric assumptions and lack of full representation of the different RV regions (often resulting in substantial underestimation of true RV volume). However, 3D measures of RV volume have largely overcome these limitations and can be obtained using 3D surface modeling platforms, starting with a full volume acquisition of the RV, the user manually identifies specified RV landmarks or contours and the proprietary software algorithm proceeds to fit a 3D model and calculate global and regional RV volumes [12].

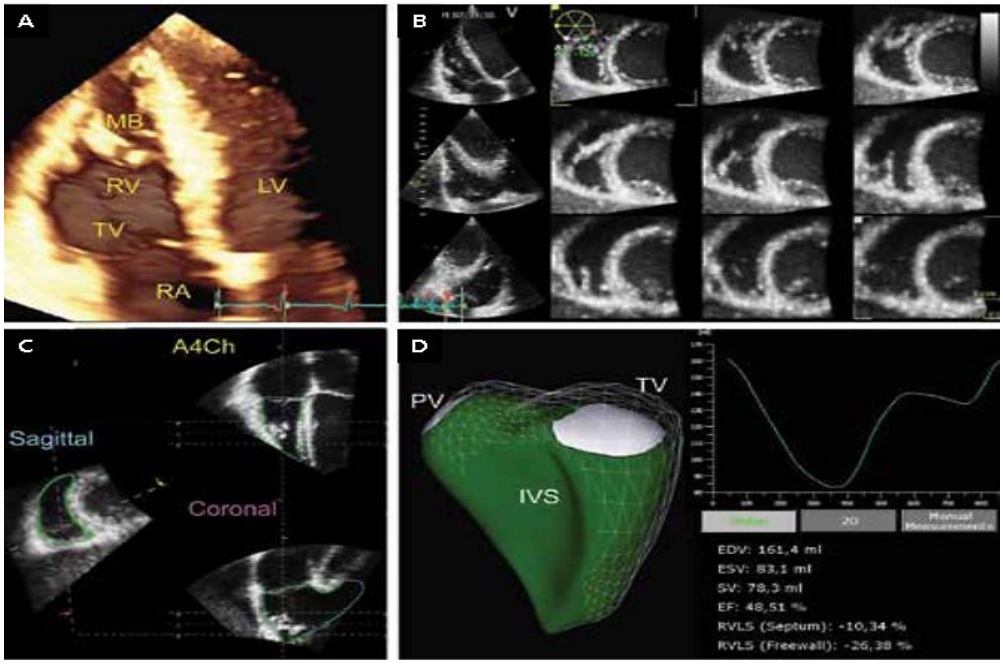

Figure (2): Display modes of a three-dimensional (3D) data set of the right ventricle (RV) obtained from the RV-focused apical four-chamber view, A. Volume rendering demonstrating the RV anatomy; B. Multi (twelve)-slice mode; C. Semiautomatic identification of the RV endocardial surface in the RV short-axis, four-chamber,

and coronal views (orthogonal planes); D. Surface rendered dynamic 3D model of the RV (green model). Global and regional RV-end diastolic and end-systolic volumes are reported, along with RV ejection fraction. [15]
Three-dimensional echocardiography-derived RV volumes achieve the closest correlation with the CMR reference standard, especially when enhanced by contrast [13].
Right Ventricular Wall Thickness:
RV hypertrophy is recognized by inspecting the wall of the RVOT in the parasternal views, the RV free wall in the apical view, and the RV inferolateral/diaphragmatic wall in the subcostal view. Generally, the RV free wall in diastole is approximately 3 to 4 mm thick; if it exceeds 5 mm, it is considered hypertrophied. Due to measurement variability, regardless of the method used, it should be noted that RV thickness by echocardiography has low sensitivity and specificity for identifying true RV hypertrophy.
Interventricular Septal Shape:
A D-shaped left ventricular cavity (also referred to as a flattened interventricular septum) in systole (particularly end-systole) suggests right ventricular (RV) pressure overload, whereas a D-shaped left ventricular cavity in diastole suggests RV volume overload [12].
Right Ventricular Function:
The predominant motion of the right ventricle (RV) is longitudinal shortening, visible as systolic descent of the basal portion of the free wall toward the apex. A secondary motion is radial thickening, visible as systolic thickening of the myocardium. Unlike the left ventricle, circumferential shortening is negligible in the RV, owing to its lack of circumferential fibers. The quantitative echocardiographic parameters used to measure RV systolic function reflect longitudinal shortening, longitudinal shortening plus inwards motion, or global RV performance [13].

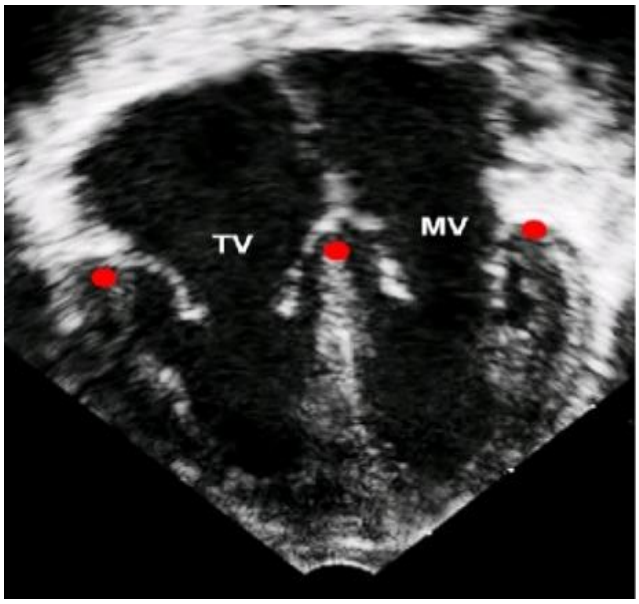

Figure (3): Apical 4 chamber view [12].
Tricuspid Annular Plane Systolic Excursion (TAPSE):
Tricuspid annular plane systolic excursion (TAPSE), sometimes referred to as tricuspid annular motion (TAM), reflects longitudinal shortening of the RV. TAPSE is measured in the apical four-chamber view by placing an M-mode cursor on the lateral tricuspid annulus and measuring the peak distance travelled by this reference point during systole. A greater distance travelled during systole implies greater RV systolic function [14].

The primary limitation of TAPSE is that it only represents one component of RV motion within one single segment of RV myocardium. The RV may be frankly dysfunctional despite relatively preserved TAPSE, as in some cases of severe pulmonary arterial hypertension. Alternatively, the RV function may be globally preserved despite significantly reduced TAPSE, as often seen after cardiac surgery. In healthy individuals, TAPSE correlates with RV size [15].

Two common sources of error with TAPSE are:

- Not placing the M-mode cursor parallel to the plane of longitudinal motion, which results in angle-dependent underestimation of TAPSE.
- Incorrectly measuring the magnitude of displacement from the M-mode image.

These issues aside, TAPSE remains one of the most widely used measures of RV systolic function since it is easily obtained and has been shown to have robust diagnostic and prognostic value in several disease states [15].

- In patients with precapillary pulmonary hypertension, TAPSE has been shown to correlate with cardiovascular magnetic resonance (CMR)-derived RV ejection fraction (RVEF) and predict long-term mortality.
- In three separate series of patients with chronic left-sided systolic heart failure, up to 50 percent of patients were found to have a reduced TAPSE, a finding that was associated with a significant increase in long-term mortality. [16]

Tricuspid Annular Velocity (TAPSE):

Also reflects the longitudinal displacement of the tricuspid annulus during systole. S' reflects the longitudinal velocity of the tricuspid annulus during systole. S' is measured in the apical four-chamber view by placing a tissue Doppler cursor on the lateral tricuspid annulus and measuring the peak velocity of this reference point during systole. Care should be taken to measure the peak of the ejection waveform and not the earlier isovolumetric contraction waveform [16].

The advantages and limitations are the same as TAPSE: S' is simple to perform and has prognostic data, yet it is angle-dependent and only represents the longitudinal annular component of RV motion. S' has been shown to correlate with CMR-derived RVEF and predicts outcomes in patients with pulmonary hypertension, chronic heart failure, and arrhythmogenic RV cardiomyopathy (ARVC) [17].

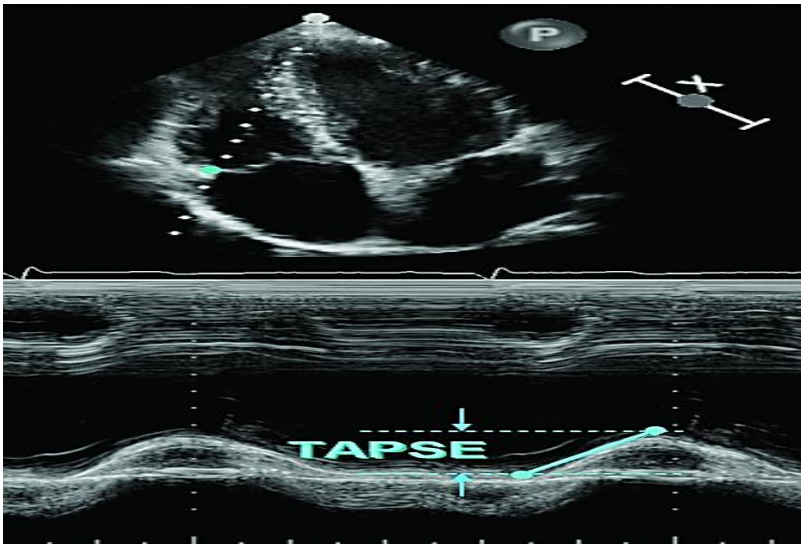

Figure (4): Tricuspid annular plane systolic excursion (TAPSE) with the normal reference limit being a TAPSE of ≥1.7 cm. [17].

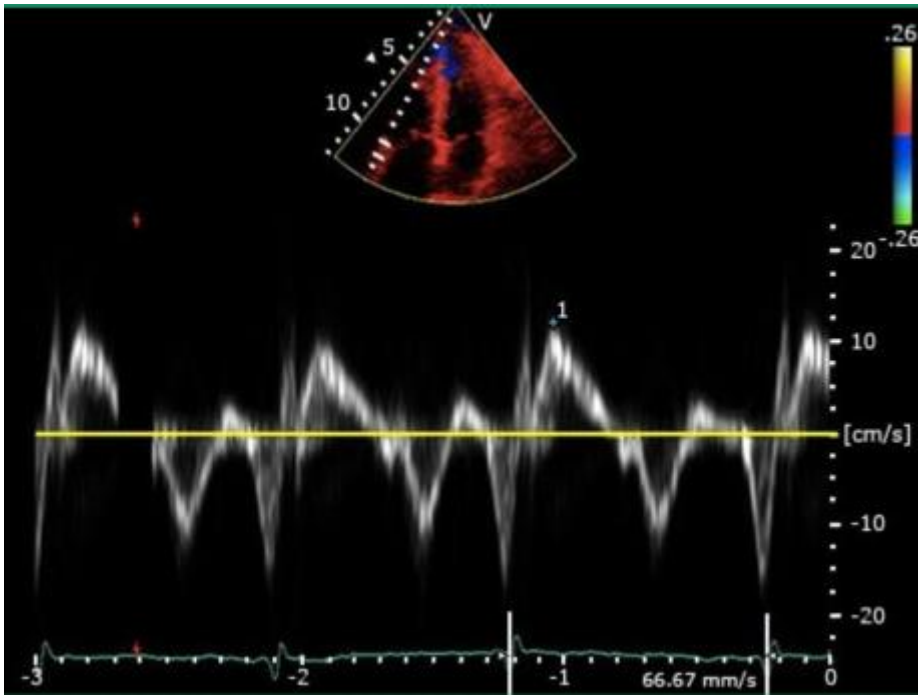

Figure (5): Tissue Doppler of the lateral tricuspid annulus obtained from the apical 4-chamber view. [17].

Fractional Area Change:

Fractional area change (FAC) is the percent change in RV area from diastole to systole, a two-dimensional surrogate for ejection fraction, and thereby reflects the systolic function of the inflow and apical portions of the RV. FAC is not limited to one type of motion, but rather encompasses longitudinal shortening as well as radial thickening and the contribution of the interventricular septum. It is measured in the apical four-chamber view by manually tracing the contour of the RV at end-diastole (when the RV cavity is at its largest) and at end-systole (when the RV cavity is at its smallest). The FAC is calculated as follows [16]:

- FAC = [(end-diastolic RV area – end-systolic RV area) / end-diastolic RV area] x 100

The normal reference limit for FAC is ≥35 percent. The primary challenge and main limitation of FAC is the accurate identification and tracing of the true RV endocardial border rather than the prominent trabeculations and muscle bands [11].

FAC appears to be an excellent compromise between efficiency of use and global representation of RV systolic function. Compared with other two-dimensional measures of RV systolic function such as TAPSE and S', FAC was found to correlate best with the reference standard of CMR-derived RVEF (R = 0.80) [18].

The revised ARVC (Arrthmiogenic right ventricular cardiomyopathy) Task Force Criteria list FAC ≤33 percent as a major diagnostic criterion and FAC 34 to 40 percent as a minor criterion (no other 2D echocardiographic measures of function were recommended) [19].

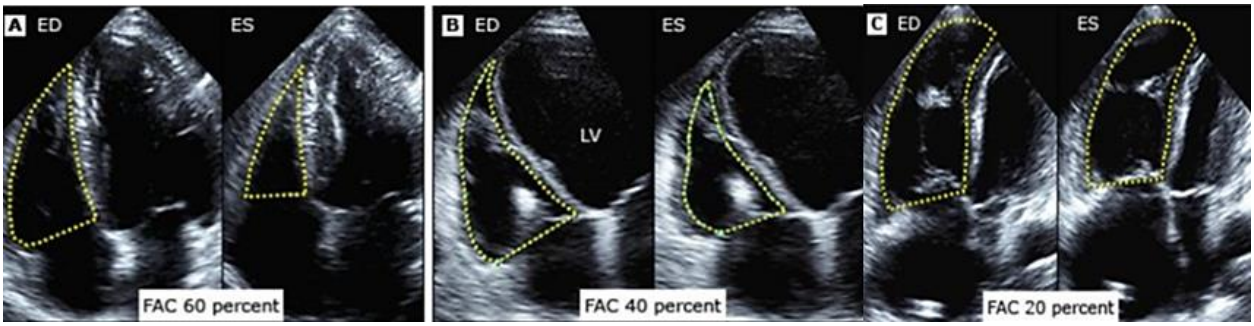

Figure (6): Right ventricular fractional area change (FAC). (A) Normal subject, FAC 60 percent. (B) Moderately dilated right ventricle (RV), FAC 40 percent. (C) Dilated RV, FAC 20 percent. [19]

Right Ventricular Ejection Fraction by 3D:

RVEF is calculated as ([end-diastolic volume – end-systolic volume] / end-diastolic RV volume), with volumes measured from a 3D acquisition. Given adequate image quality, 3D-derived RVEF using either the method of discs or surface modeling is the most accurate echocardiographic measure of global RV systolic function. A study of 507 normal subjects has provided reference values for both genders of various age decades. In general, the normal reference limit for 3D-derived RVEF is ≥45 percent [20].

Strain

Strain is defined as the percent change in myocardial deformation (predominantly longitudinal shortening in the case of the RV). Strain is currently measured principally by the speckle-tracking (non-angle-dependent) approach. Potential pitfalls include technical challenges in image acquisition and analysis (need for high frame rates, minimal image dropout, experienced observers for reproducible measurements) as well as inter-vendor variability [21].

The normal reference limit for speckle-tracking strain of the RV free wall is -23 percent (with more negative values indicating better function) [22].

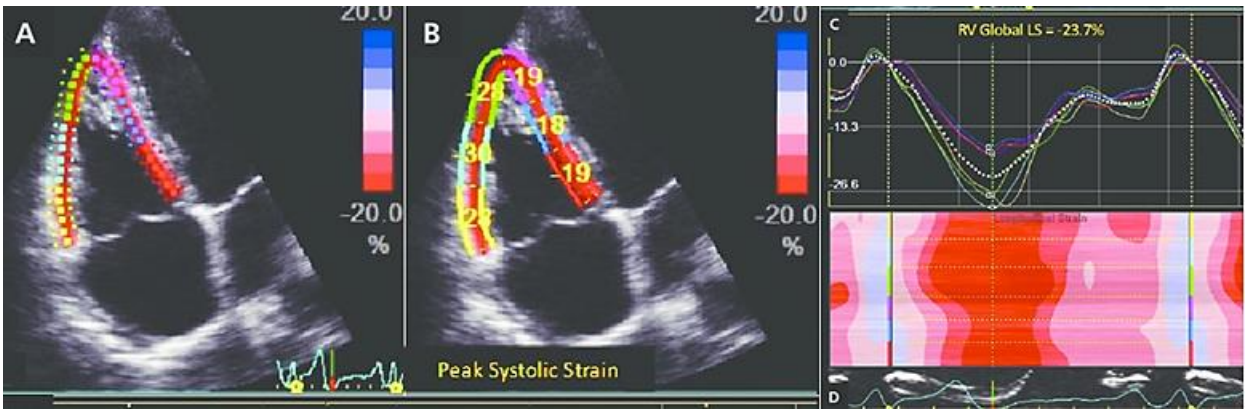

Figure (7) : Peak systolic longitudinal strain (LS) of the right ventricular (RV) free wall and interventricular septum obtained with 2D speckle-tracking analysis; A. end-systolic strain; B. end-systolic strain; C. Strain-time curves during the cardiac cycle; D. Anatomical M-mode color-coded display of segmental strain variations during the cardiac cycle. [15]

Pulmonary Hypertension in Children

Common Types of Pulmonary Hypertension (PH) in Children:

Definition:

For children and infants >3 months old, the definition of PH is the same as in adults: mean pulmonary artery pressure (PAP) >20 mmHg at sea level [25].

Clinical Classification of Pulmonary Hypertension (6th World Symposium on Pulmonary Hypertension)

1. Primary Pulmonary arterial hypertension
2. PH due to left heart disease
3. PH due to lung disease and/or hypoxia
4. PH due to pulmonary artery obstructions
5. PH with unclear and/or multifactorial mechanisms [25].

Virtually all types of PH in this classification can be observed in pediatric patients. The most common types of persistent/progressive PH in children are PH associated with congenital heart disease, PH due to lung disease, and idiopathic/heritable PH [25].

Transient forms of PH, such as persistent PH of the newborn (PPHN) and PH related to congenital diaphragmatic hernia, are also relatively common [20].

PH is well described in children with collagen vascular disease, liver disease, and acute thromboembolism, but these diseases are rare causes of PH in children [21].

Persistent Pulmonary Hypertension of the Newborn – Mostly Transient

Congenital Heart Disease –

Only a small minority of patients with congenital heart disease develop clinically significant PH. The two broad categories of congenital heart disease that can cause PH include shunting lesions and left heart disease associated with elevated left atrial pressure (LAp) [22].

Systemic-to-Pulmonary Shunting –

One of the complications of unrepaired high-pressure left to right shunting defects is that, during the first few years, the patient may develop high pulmonary vascular resistance (PVR) and pulmonary hypertensive vascular disease, which can be irreversible and progressive, which can persist and increase in patients even after closure of intracardiac shunts when closed late [22].

If PVR increases to systemic or greater levels, unrepaired defects that are typically acyanotic (eg, ventricular septal defect, patent ductus arteriosus, atrial septal defect) may become cyanotic by virtue of shunt reversal. This is referred to as Eisenmenger syndrome. Timely repair of high-pressure shunting defects is therefore of great importance [25].

Lung Diseases Causing Pulmonary Hypertension in Children –

In bronchopulmonary dysplasia, PH can be caused by acquired injury and maldevelopment of pulmonary blood vessels, and the vascular bed is especially prone to vasoconstriction with viral infection or other stresses [26]. Most patients with PH due to bronchopulmonary dysplasia are only mildly to moderately affected, especially when healthy, and PAP generally falls with growth and development. However, when PH is severe and persistent in this patient population, it is associated with considerable morbidity and mortality [26].

Many other types of acute and chronic lung disease in children may be complicated by PH, congenital diaphragmatic hernia, Interstitial lung disease, Acute respiratory distress syndrome, Pneumonia, and Cystic fibrosis [26].

Left Heart Disease –

Conditions that increase left atrial pressure (LAp) (eg, mitral valve disease, noncompliance of the left ventricle), can also cause PH; however, these are not common in childhood [14].

Pulmonary Vein Stenosis –

Pulmonary vein stenosis is a rare disease that may be idiopathic or may be associated with total or partial anomalous pulmonary venous return or prematurity. This form of PH is almost entirely unique to pediatric patients, with young infants most commonly affected [26].

Measurement of Pulmonary Artery Pressure

Echocardiographic Evaluation of Pulmonary Artery Pressure:

Right atrial pressure (RAP) is most commonly estimated based on the diameter and degree of collapse of the inferior vena cava (IVC) imaged from the subcostal view during quiet inspiration [27]:

- IVC dilation suggests increased central venous pressure and may accompany volume overload states but IVC diameter in pediatric showed a wide variation in the absolute values of IVC diameter with age in paediatric population, hence relying on IVC diameter for volume status assessment was difficult in paediatric population.
- IVC collapsibility (in spontaneously breathing patients) and IVC distensibility (in mechanically ventilated patients) is more reliable in paediatrics and has no correlation with either age or sex.

The IVC collapsibility index is calculated by the following formula: IVC collapsibility index = [maximum diameter on expiration – (minimum diameter on inspiration/ maximum diameter on expiration)] [15]. In mechanically ventilated patients, the IVC distensibility index is calculated using the formula: IVC distensibility index = [(maximum diameter on inspiration –minimum diameter on expiration)/ minimum diameter on expiration] [16].

- Normal IVC collapsibility index >50%, for IVC and distensibility index >18%, a blunted or absent inspiratory variation of IVC diameter suggests increased RA pressure [17].

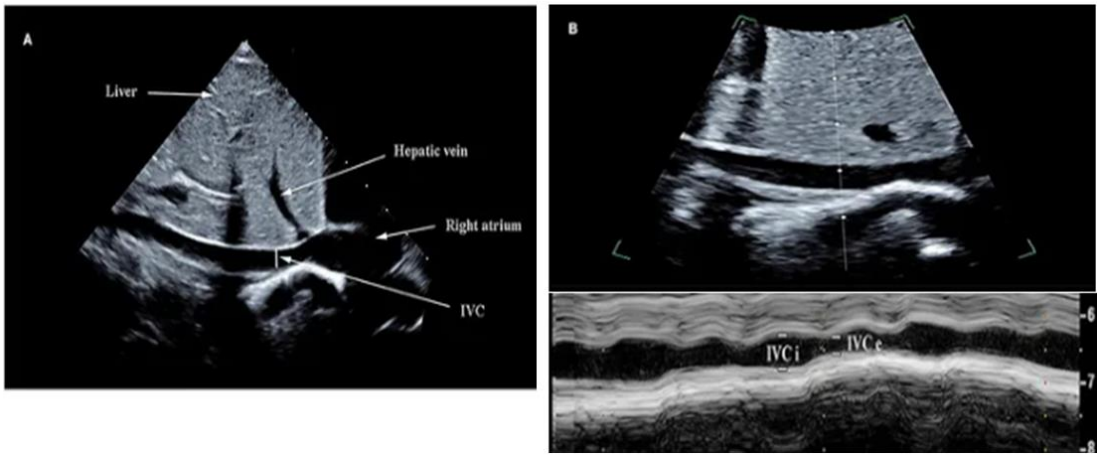

Figure (8): Ultrasonographic measurement of inferior vena cava (IVC) diameters. The IVC images were obtained using the 2D mode on a subcostal long-axis view (A). M-mode line was placed through the IVC 1–2 cm caudal from the hepatic vein-IVC confluence and an M-mode tracing obtained. The IVC maximum diameter (IVCmax) and IVC diameter (IVCmin) was measured during the respiratory cycle (B). [18].

The interpreter, however, may upgrade or downgrade the intermediate RAP value based on secondary indices that suggest either normal or elevated RAP such as RA enlargement, right ventricular (RV) hypertrophy, diastolic predominance in the hepatic veins, restrictive filling pattern in the trans-tricuspid inflow, or tricuspid E/e' >6 [29].

Pulmonary Artery Pressure:

Estimation of Pulmonary Artery Systolic Pressure:

Estimation of pulmonary artery pressure (PAP) is based on the simplified Bernoulli equation, $\Delta P = 4V2$, estimates the pressure gradient between two chambers (ΔP) based on the peak velocity (V) in the presence of turbulent flow. Thus, the gradient estimated by the peak TR velocity (TRV) measured by continuous wave Doppler is equal to the systolic pressure in the RV (RVSP) minus the systolic pressure in the RA (RAP). RVSP is equivalent to pulmonary artery systolic pressure (PASP) in the absence of an RV outflow gradient (such as with pulmonic stenosis) [29].

PASP ≈ RVSP = 4(peak TRV2) + RAP

Careful acquisition and interpretation of Doppler TRV and RAP data are required for accurate estimation of RVSP and PASP. Studies have documented a strong correlation between echocardiographic estimates and right heart catheterization measurements of PASP [30].

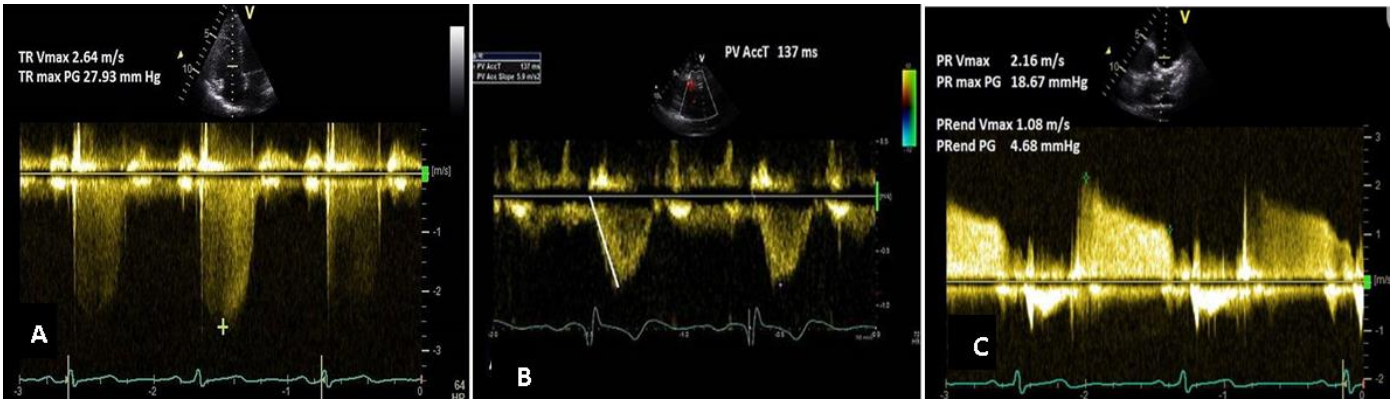

Figure (9): (A) Continuous wave Doppler showing tricuspid regurgitation (TR) (B) RVOT acceleration time method for assessing pulmonary pressure (C) pulmonary regurgitation velocity to estimate mean and diastolic pulmonary artery pressures. [21]

Other Measures of Pulmonary Artery Pressure:

Echocardiography can also be used to estimate mean and diastolic pulmonary artery pressures, using either the tricuspid or pulmonary regurgitation velocity, or the acceleration time (time to reach peak velocity in the distal RVOT flow tracing measured by pulsed wave Doppler), as follows:

- Mean PAP = 79 – [(0.45) (Acceleration time)].
- Mean PAP = VTI of the TR jet + RAP.
- Mean PAP = 0.61 x PASP + 2.
- Systolic PAP = 10[(-0.004)(Acceleration time) + 2.1] [31].

Pulmonary Vascular Resistance:

The determinants of pressure are flow and resistance, according to the formula P = QR, where pressure (P) is equal to the product of flow (Q) and resistance (R). There are situations whereby stroke volume is markedly increased, without an increase in pulmonary vascular resistance (PVR). The PASP may therefore be elevated, but the pathological or clinical implications are not the same as in the setting of increased resistance. By using a measure of flow (velocity time integral [VTI] of the RVOT) and a measure of pressure (TRV), a simple regression formula can be used to estimate PVR [32].

PVR = [(TRV / RVOT VTI) x 10] + 0.16

This yields a value in Wood units (WU), and maintains a good correlation with invasively measured PVR up to approximately 8 WU [33].

A subsequent refinement showed that PVR = (5.19 x TR Vmax2 / RVOT VTI) – 0.4 performed better, especially when PVR exceeded 6 WU; this measure should not replace invasive hemodynamic measurements [32].

Other Findings:

There are several other ancillary findings that should be used to assess for RV overload. A D-shaped left ventricular cavity in systole suggests RV pressure overload. Mid-systolic notching of the RVOT pulsed wave Doppler flow signal or pulmonary valve M-mode signal suggests increased PVR. This finding reflects a prominent reflected wave, and has been used to refine estimates of PVR using the formula: PVR = (PASP/ RVOT VTI) + 3 if a mid-systolic notching of the RVOT is present [34].

Cardiac Catheterization:

Cardiac catheterization is the gold standard for diagnosis of PH:

Indications:

- Cardiac catheterization should generally be performed prior to initiation of targeted PH therapy,
- When noninvasive testing is inadequate or nondiagnostic
- Follow-up of patients on targeted therapy
- In patients with systemic-to-pulmonary shunts to assess operability (although this is infrequently required, especially in the first year of life)
- In patients undergoing evaluation for heart or heart-lung transplantation to assess suitability for transplantation [35].

Information Provided by Catheterization – Compared with echocardiography, cardiac catheterization:

- Provides a more accurate measurement of PAP
- Provides additional hemodynamic measurements (eg, cardiac output, atrial pressures, pulmonary capillary wedge pressure)
- Allows vasoreactivity testing (ie, measurement of the response to vasodilators, such as inhaled nitric oxide)
- Allows measurement of flow through shunt lesions
- In some cases, interventions can be performed to close shunting lesions (eg, device closure of atrial septal defect, coiling of aortopulmonary collaterals)
- Can demonstrate abnormally shaped and distributed pulmonary arteries or stenosis of large pulmonary arteries [36].

Acute Vasoreactivity Testing (AVT) –

AVT is a particularly important component of the cardiac catheterization in children with PH as it informs prognosis and can guide therapy (eg, reactive patients are often treated with calcium channel blockers) [37].

Acute vasoreactivity testing (AVT) involves the administration of a short-acting vasodilator (typically inhaled nitric oxide) followed by measurement of the hemodynamic response [37].

The Pediatric Task Force of the 2018 6th World Symposium on Pulmonary Hypertension (WSPH) suggested that "reactivity" be defined by a decrease in mean PAP by at least 10 mmHg to a value of <40 mmHg with no decrease in cardiac output. Other alternative criteria define reactivity as a ≥20 percent decrease in mean PAP with a decreased ratio of systemic to pulmonary vascular resistance (PVR) and unchanged or increased cardiac index [35].

Careful evaluation of right ventricular function is paramount in assessing the cause of pulmonary hypertension and severity of disease. Further, it has prognostic significance, as many representative parameters of right ventricular function have been linked with mortality. In our opinion, right ventricular function should be assessed serially throughout the course of treatment in pulmonary hypertension, and baseline parameters in addition to dynamic changes should be incorporated into risk assessment. Achieving normal or near-normal right ventricular performance may serve as a principal goal in the treatment of pulmonary hypertension.

References

1. Bhalla, A., Baudin, F., Takeuchi, M., Cruces, P., Second Pediatric Acute Lung Injury Consensus Conference (PALICC-2) of the Pediatric Acute Lung Injury and Sepsis Investigators (PALISI) Network. Monitoring in pediatric acute respiratory distress syndrome: from the second Pediatric Acute Lung Injury Consensus Conference. Pediatric Critical Care Medicine, 24(S1), S112–S123.

2. Emeriaud, G., Lopez-Fernandez, Y. M., Iyer, N. P., Bembea, M. M., Agulnik, A., Barbaro, R. P., et al. Executive summary of the second international guidelines for the diagnosis and Management of Pediatric Acute Respiratory Distress Syndrome (PALICC-2). Pediatric Critical Care Medicine, 24(2), 143–168.
3. Ganeriwal, S., Alves Dos Anjos, G., Schleicher, M., Hockstein, M. A., Tonelli, A. R., Duggal, A., et al. Right ventricle-specific therapies in acute respiratory distress syndrome: a scoping review. Critical Care, (2023), 27, 104.
4. Kovács, A., Lakatos, B., Tokodi, M., et al. Right ventricular mechanical pattern in health and disease: beyond longitudinal shortening. Heart Failure Reviews, 24, 511–520 (2019).
5. Babaie, S., Behzad, A., Mohammadpour, M., & Reisi, M. (2018). A comparison between the bedside sonographic measurements of the inferior vena cava indices and the central venous pressure while assessing the decreased intravascular volume in children. Advances in Biomedical Research, 7, 97.
6. Lujan Varas, J., Martinez Díaz, C., Blancas, R., Martnez Gonzalez, O., Llorente Ruiz, B., Molina Montero, R., et al. Inferior vena cava distensibility index predicting fluid responsiveness in ventilated patients. Intensive Care Medicine Experimental, 3(Suppl 1), A600.
7. Yildizdas, D., & Aslan, N. (2020). Ultrasonographic inferior vena cava collapsibility and distensibility indices for detecting the volume status of critically ill pediatric patients. Journal of Ultrasonography, 20, e205–e209.
8. Xiong, Z., Zhang, G., Zhou, Q., Lu, B., Zheng, X., Wu, M., & Qu, Y. (2022). Predictive Value of the Respiratory Variation in Inferior Vena Cava Diameter for Ventilated Children With Septic Shock. Frontiers in Pediatrics, 10, 895651.
9. Greyson, C. R. (2010). Ventrículo derecho y circulación pulmonar: conceptos básicos. Revista Española de Cardiología (English Edition), 63(1), 81-95.
10. Baum, V. C., & Palmisano, B. W. (1997). The immature heart and anesthesia. Anesthesiology, 87(6), 1529–1548.
11. Haddad, F., Hunt, S. A., Rosenthal, D. N., & Murphy, D. J. (2008). Right ventricular function in cardiovascular disease, part I: anatomy, physiology, aging, and functional assessment of the right ventricle. Circulation, 117(14), 1436–1448.
12. Singh, S., White, F. C., & Bloor, C. M. (1981). Myocardial morphometric characteristics in swine. Circulation Research, 49(2), 434–441.
13. Woulfe, K. C., & Walker, L. A. (2021). Physiology of the right ventricle across the lifespan. Frontiers in Physiology, 12, 642284.
14. Webb, L., Burton, L., Manchikalapati, A., Prabhakaran, P., Loberger, J. M., & Richter, R. P. (2023). Cardiac dysfunction in severe pediatric acute respiratory distress syndrome: the right ventricle in search of the right therapy. Frontiers in Medicine, 10, 1216538.
15. Surkova, Elena & Peluso, Diletta & Kasprzak, Jaroslaw & Badano, Luigi. (2016). Use of novel echocardiographic techniques to assess right ventricular geometry and function. Kardiologia polska, 74.
16. Lujan Varas, J., Martinez Díaz, C., Blancas, R., Martnez Gonzalez, O., Llorente Ruiz, B., Molina Montero, R., et al. (2015). Inferior vena cava distensibility index predicting fluid responsiveness in ventilated patients. Intensive Care Medicine Experimental, 3(Suppl 1), A600.
17. Parasuraman, S., Walker, S., Loudon, B. L., Gollop, N. D., Wilson, A. M., Lowery, C., & Frenneaux, M. P. (2016). Assessment of pulmonary artery pressure by echocardiography-A comprehensive review. International Journal of Cardiology and Heart Vascular, 12, 45-51.
15. Babaie, S., Behzad, A., Mohammadpour, M., & Reisi, M. (2018). A comparison between the bedside sonographic measurements of the inferior vena cava indices and the central venous pressure while assessing the decreased intravascular volume in children. Advances in Biomedical Research, 7, 97.
16. Lujan Varas, J., Martinez Díaz, C., Blancas, R., Martnez Gonzalez, O., Llorente Ruiz, B., Molina Montero, R., et al. (2015). Inferior vena cava distensibility index predicting fluid responsiveness in ventilated patients. Intensive Care Medicine Experimental, 3(Suppl 1), A600.

17. Yildizdas, D., & Aslan, N. (2020). Ultrasonographic inferior vena cava collapsibility and distensibility indices for detecting the volume status of critically ill pediatric patients. Journal of Ultrasonography, 20, e205–e209.
18. Xiong, Z., Zhang, G., Zhou, Q., Lu, B., Zheng, X., Wu, M., & Qu, Y. (2022). Predictive Value of the Respiratory Variation in Inferior Vena Cava Diameter for Ventilated Children With Septic Shock. Frontiers in Pediatrics, 10, 895651.
19. Rudski, L. G., Lai, W. W., Afilalo, J., et al. (2010). Guidelines for the echocardiographic assessment of the right heart in adults: a report from the American Society of Echocardiography endorsed by the European Association of Echocardiography, a registered branch of the European Society of Cardiology, and the Canadian Society of Echocardiography. Journal of the American Society of Echocardiography, 23, 685-713.
20. Maffessanti, F., Muraru, D., Esposito, R., et al. (2013). Age-, body size-, and sex-specific reference values for right ventricular volumes and ejection fraction by three-dimensional echocardiography: a multicenter echocardiographic study in 507 healthy volunteers. Circulation: Cardiovascular Imaging, 6, 700.
21. Parasuraman, S., Walker, S., Loudon, B. L., Gollop, N. D., Wilson, A. M., Lowery, C., & Frenneaux, M. P. (2016). Assessment of pulmonary artery pressure by echocardiography-A comprehensive review. International Journal of Cardiology and Heart Vascular, 12, 45-51.
22. El–Saied, M. M., Mohie El Deen, Z. M., & Askar, G. A. (2019). Recurrent pneumonia in children admitted to Assiut university children hospital. Magnitude of the problem and possible risk factors. Medical Research Journal, 4(1), 13-24.
23. Malloy, K. W., & Austin, E. D. (2021). Pulmonary hypertension in the child with bronchopulmonary dysplasia. Pediatric Pulmonology, 56(11), 3546-3556.
24. Beigel, R., Cercek, B., Luo, H., et al. (2013). Noninvasive evaluation of right atrial pressure. Journal of the American Society of Echocardiography, 26, 1033.
25. Rosenzweig, E. B., Abman, S. H., Adatia, I., et al. (2019). Paediatric pulmonary arterial hypertension: Updates on definition, classification, diagnostics and management. European Respiratory Journal, 53, 1801949.
26. Do, D. H., Therrien, J., Marelli, A., et al. (2011). Right atrial size relates to right ventricular end-diastolic pressure in an adult population with congenital heart disease. Echocardiography, 28, 109.
27. Amsallem, M., Sternbach, J. M., Adigopula, S., et al. (2016). Addressing the Controversy of Estimating Pulmonary Arterial Pressure by Echocardiography. Journal of the American Society of Echocardiography, 29, 93.
28. Yared, K., Noseworthy, P., Weyman, A. E., et al. (2011). Pulmonary artery acceleration time provides an accurate estimate of systolic pulmonary arterial pressure during transthoracic echocardiography. Journal of the American Society of Echocardiography, 24, 687.
29. Abbas, A. E., Franey, L. M., Marwick, T., et al. (2013). Noninvasive assessment of pulmonary vascular resistance by Doppler echocardiography. Journal of the American Society of Echocardiography, 26, 1170.
30. Rajagopalan, N., Simon, M. A., Suffoletto, M. S., et al. (2009). Noninvasive estimation of pulmonary vascular resistance in pulmonary hypertension. Echocardiography, 26, 489.
31. Opotowsky, A. R., Clair, M., Afilalo, J., et al. (2013). A simple echocardiographic method to estimate pulmonary vascular resistance. The American Journal of Cardiology, 112, 873.
32. Rajagopalan, N., Simon, M. A., Suffoletto, M. S., et al. (2009). Noninvasive estimation of pulmonary vascular resistance in pulmonary hypertension. Echocardiography, 26, 489.
33. Kulik, T. J., Clark, R. L., Hasan, B. S., et al. (2011). Pulmonary arterial hypertension: what the large pulmonary arteries tell us. Pediatric Cardiology, 32, 759.
34. Douwes, J. M., van Loon, R. L., Hoendermis, E. S., et al. (2011). Acute pulmonary vasodilator response in paediatric and adult pulmonary arterial hypertension: occurrence and prognostic value when comparing three response criteria. European Heart Journal, 32, 3137.
35. Rosenzweig, E. B., Abman, S. H., Adatia, I., et al. (2019). Paediatric pulmonary arterial hypertension: Updates on definition, classification, diagnostics and management. European Respiratory Journal, 53, 1801949.

36. Opotowsky, A. R., Clair, M., Afilalo, J., et al. (2013). A simple echocardiographic method to estimate pulmonary vascular resistance. The American Journal of Cardiology, 112, 873.
37. Rosenzweig, E. B., Abman, S. H., Adatia, I., et al. (2019). Paediatric pulmonary arterial hypertension: Updates on definition, classification, diagnostics and management. European Respiratory Journal, 53, 1801949.
38. Lai, W. W., Gauvreau, K., Rivera, E. S., et al. (2008). Accuracy of guideline recommendations for two-dimensional quantification of the right ventricle by echocardiography. International Journal of Cardiovascular Imaging, 24, 691.
39. Leibundgut, G., Rohner, A., Grize, L., et al. (2010). Dynamic assessment of right ventricular volumes and function by real-time three-dimensional echocardiography: a comparison study with magnetic resonance imaging in 100 adult patients. Journal of the American Society of Echocardiography, 23, 116.
40. Medvedofsky, D., Mor-Avi, V., Kruse, E., et al. (2017). Quantification of Right Ventricular Size and Function from Contrast-Enhanced Three-Dimensional Echocardiographic Images. Journal of the American Society of Echocardiography, 30, 1193.
41. Lang, R. M., Badano, L. P., Mor-Avi, V., et al. (2015). Recommendations for cardiac chamber quantification by echocardiography in adults: an update from the American Society of Echocardiography and the European Association of Cardiovascular Imaging. Journal of the American Society of Echocardiography, 28, 1.
42. Ferrara, F., Rudski, L. G., Vriz, O., et al. (2016). Physiologic correlates of tricuspid annular plane systolic excursion in 1168 healthy subjects. International Journal of Cardiology, 223, 736.
43. Sato, T., Tsujino, I., Ohira, H., et al. (2012). Validation study on the accuracy of echocardiographic measurements of right ventricular systolic function in pulmonary hypertension. Journal of the American Society of Echocardiography, 25, 280.
44. Liu, Y. T., Li, M. T., Fang, Q., et al. (2012). Right-heart function related to the results of acute pulmonary vasodilator testing in patients with pulmonary arterial hypertension caused by connective tissue disease. Journal of the American Society of Echocardiography, 25, 274.
45. Anavekar, N. S., Gerson, D., Skali, H., et al. (2007). Two-dimensional assessment of right ventricular function: an echocardiographic-MRI correlative study. Echocardiography, 24, 452.
46. Marcus, F. I., McKenna, W. J., Sherrill, D., et al. (2010). Diagnosis of arrhythmogenic right ventricular cardiomyopathy/dysplasia: proposed modification of the task force criteria. Circulation, 121, 1533.
47. López-Candales, A., Rajagopalan, N., Dohi, K., et al. (2007). Abnormal right ventricular myocardial strain generation in mild pulmonary hypertension. Echocardiography, 24, 615.
48. Badano, L. P., & Muraru, D. (2016). Subclinical Right Ventricular Dysfunction by Strain Analysis: Refining the Targets of Echocardiographic Imaging in Systemic Sclerosis. Circulation: Cardiovascular Imaging, 9.